Medicinska istraživanja 2026 | DOI: 10.5937/medi0-64148

OPEN ACCESS

Medical Research | Published by Faculty of Medicine University of Belgrade

REVIEW ARTICLE

CT perfusion in oncological imaging

Aleksandra Djuric-Stefanovic[1,2], Milica Mitrovic Jovanovic[1,2], Jelena Kovac[1,2], Aleksandar Ivanovic[1,2], Slavenko Ostojic[1,3], Nikica Grubor[1,3], Dejan Stojakov[1,4], Predrag Sabljak[1,3]

[1]University of Belgrade, Faculty of Medicine, Belgrade, Serbia
[2]University Clinical Center of Serbia, Center of Radiology, Department of Digestive Radiology, Belgrade, Serbia
[3]University Clinical Center of Serbia, Clinic of Digestive Surgery (First University Surgical Clinic), Belgrade, Serbia
[4]Clinical Hospital Center "Dr Dragiša Mišović", Clinic of Surgery, Belgrade, Serbia

Submitted: 17 January 2026
Revised: 18 March 2026
Accepted: 20 March 2026
Online First: 30 March 2026

Check for updates

Correspondence to:
Aleksandra Djuric-Stefanovic
University Clinical Center of Serbia, Center of Radiology, Department of Digestive Radiology (First Surgery University Clinic)
6 Koste Todorovica Street, 11000 Beograd, Serbia
Email: aleksandra.djuricstefanovic@gmail.com

Summary

Computed tomography (CT) perfusion is a CT examination modality that enables visualization and non-invasive quantitative assessment of tissue perfusion. Application of CT perfusion in oncology enables non-invasive detection and quantification of neo-angiogenesis (i. e., pathological vascularization) in various malignant tumors. Based on the values of CT perfusion parameters, it is possible to distinguish neoplastic from healthy tissue, malignant from benign tumors, highly aggressive from low-aggressive tumors, and good from poor tumor response to oncological therapy. The basic principle of low-dose CT perfusion is to repeatedly scan the selected region where the tumor is located, using reduced tube voltage and current, at short time intervals after intravenous administration of a small bolus of iodine contrast by an automatic injector at a high flow rate. Using different kinetic-mathematical models allows measurement of certain tissue perfusion parameters, including: blood flow (BF), circulating blood volume (BV), mean transit time (MTT), and vascular permeability (PS or K trans). While results from different CT perfusion software are not comparable, the standardized perfusion value (SPV) is a universal semi-quantitative indicator of tissue perfusion that is independent of the CT perfusion algorithm and can be easily calculated without commercial CT perfusion software. While BF, BV, and PS values are significantly higher in the majority of high-grade malignant tumors compared to low-grade or benign tumors or healthy tissue, MTT is often lower in high-grade tumors. A significant decline in CT perfusion parameter values is a marker of a good response of the neoplasm to the oncological therapy.

Keywords: CT perfusion, imaging, oncology, CT

Cite this article as: Djuric-Stefanovic A, Mitrovic Jovanovic M, Kovac J, Ivanovic A, Ostojic S, Grubor N. et al. DCT perfusion in oncological imaging; Medicinska istraživanja 2026; DOI: 10.5937/medi0-64148

INTRODUCTION

Computed tomography (CT) perfusion, i.e., DCE-CT (dynamic contrast-enhanced computed tomography), is an imaging modality that enables non-invasive quantitative assessment of tissue perfusion, thereby introducing functional diagnostic elements into morphological imaging (1-4). Repeated CT scanning of the selected region after intravenous administration of an iodine contrast agent at a fixed time interval enables dynamic monitoring of contrast enhancement in blood vessels and tissues. After applying certain mathematical algorithms, which can be incorporated into commercial or freely available CT perfusion software, the perfusion of all tissues in the scanned region can be determined (1-7).

The clinical application of CT perfusion was developing in two directions: the diagnosis of ischemic lesions and oncologic diagnosis (1-12). In the diagnosis of ischemic lesions, the role of CT perfusion is to discriminate necrosis, an irreversible consequence of ischemia, from the surrounding reversible zone of ischemia (penumbra) (2, 7-12). It is used to assess the volumes of necrosis and penumbra in ischemic lesions of the brain, heart, and pancreas in acute pancreatitis (7-12).

The application of CT perfusion in oncology diagnostics enables the non-invasive detection and quantification of neovascularization (i.e., pathological vascularization) in various malignant tumors (1-5). In this review, we present how to incorporate CT perfusion into the diagnostic process for oncological patients, along with its strengths and limitations. With certain limitations that should be overcome, CT perfusion is ready for clinical use in oncologic imaging.

METHODOLOGY

For this narrative review, we searched the PubMed database for studies on the use of CT perfusion in oncology diagnostics published in English between 1980 and 2025.

CT PERFUSION IN ONCOLOGY

History and development of CT perfusion

In 1980, Leon Axel was the first to propose a method of quantitative assessment of blood flow in brain tissue by CT (13). This technique was based on continuous monitoring of changes in tissue density during and after intravenous administration of iodine contrast medium (13, 14). In 1993, Miles et al. published the first paper on the extra-cerebral application of CT perfusion in the assessment of liver perfusion (15). Due to the technical limitations of the first generations of CT machines, including long scanning times per section and the ability to repeatedly scan only one section, the CT perfusion technique was widely adopted only with the advent of the new generation of CT. The introduction of spiral single-slice CT enabled satisfactory scanning speeds (e.g., one slice per second) for reliable monitoring of post-contrast tissue attenuation dynamics. However, repeated scanning was still limited to a maximum of 10 mm-thick slices per rotation, which usually covers only a small part of the tumor (1-4). The introduction of a new generation of multi-detector CT (MDCT) devices into clinical practice enabled visualization of tumor perfusion throughout the tumor or even the whole organ, depending on the number of CT detectors **(Table 1)** (1-5).

Table 1. CT perfusion protocols on different CT scanners

Type of CT	64-MDCT (LightSpeed, GE) (16, 26, 60-63)	64-MDCT (Aquilion, Toshiba) (45, 59)	128-MDCT (Aquilion, Toshiba) (74)
Mode	Cine	Cine	Axial (Intermittent)
Slice thickness	5 mm	8 mm	5 mm
No of slices	8	4	32
Z-axis coverage	40 mm	32 mm	160 mm
Repetition time	1 s	2 s	1 s/2 s/3 s/5 s (wait: 6.5, 2.5, 4.5 s)
Scan duration	50 s	50 s	64 s
No of series	50	21	21 (1/9/6/5)
Total No of images	400	104	672
Scan delay	5 s	5 s	7 s
Breathing	Free	Free	Breath holding
Tube voltage	80 kV	100 kV	100 kV
Tube current	40 mAs	50 mAs	30 mAs
Volume of contrast (350 or 370 mg I/ml) + 9% NaCl	50 + 50 ml	50 + 50 ml	50 + 50 ml
Flow rate	≥4 ml/s	≥4 ml/s	≥4 ml/s
Effective dose of radiation	2.84 mSv	4.45 mSv	10.68 mSv

Abbreviations: MDCT - multi-detector computed tomography; mm - millimeters; s - seconds; kV - kilovolts; mAs - milliamperseconds; ml - milliliters; mSv - milliSiverts; I - iodine; NaCl - sodium chloride

CT perfusion technique

CT perfusion involves repeated scanning of a selected region where the tumor is located at short time intervals (1-2 s), for at least 45-50 s, after intravenous administration of a bolus of iodine contrast by automatic injector with a high flow rate **(Table 1)** (1-4). Before the contrast is injected, a non-contrast low-dose image limited to the tumor region is obtained to plan the CT perfusion study. The volume of the scanned region, the repetition time, and the flow rate are determined by the technical capabilities of the CT scanner and available CT perfusion software **(Table 1)** (1-4).

Analysis of the CT perfusion study

The analysis of a CT perfusion study always begins by placing a circular ROI (region of interest) in the center of the largest adjacent arterial blood vessel, whereby an arterial time-density curve is automatically obtained, which shows the dynamics of the density change in the artery as a function of time **(Figure 1a, c)**. At the same time, a CT perfusion parameter map is obtained for the entire scanned volume **(Figure 1e-h)**. The tumor's outer borders are then drawn using a freehand or oval ROI. Usually, another ROI is placed in the region of adjacent healthy tissue of the organ from which the tumor originated, or another reference organ or tissue (most often the skeletal muscle) **(Figure 1b)**. Thus, quantitative values for all available CT perfusion parameters of the tumor and the reference healthy tissue are presented on the reconstructed view of each consecutive section within the scanned volume **(Figure 1e-h)**.

The reconstructed view of each section (reference image) is a fused, unified view of all cross-sections sequentially scanned over a given time at the same coordinate range, obtained by software reconstruction that corrects artifacts caused by patient movement and breathing **(Figure 1b)**. After marking the ROI of the tumor and reference healthy tissue, an arterial, tumor, and healthy tissue time-density curve is obtained, which shows the dynamics of changes in density in the artery, tumor, and reference healthy tissue as a function of time in the same coordinate system **(Figure 1c, d)**. At the same time, automatically calculated values of perfusion parameters for each marked ROI of tumor and reference healthy tissue (mean value and SD) are displayed on already existing perfusion maps **(Figure 1e-h)**.

CT perfusion parameters

By applying several kinetic-mathematical models, various software for CT perfusion were developed, which allowed the measurement of the following tissue perfusion parameters **(Figures 1-5)** (1-4):

Blood flow (BF): blood flow rate per unit volume or mass of tissue [ml/min/100ml]

Blood volume (BV): volume of circulating blood per unit volume or mass of tissue [ml/100ml]

Mean transit time (MTT): the average time for the contrast to pass through the tissue vascular network [s]

Capillary permeability surface area product (PS): the ratio of the diffusion rate of the contrast medium through the capillary endothelial and the total surface area of the capillary endothelial [ml/min/100ml] (Deconvolution kinetic model)

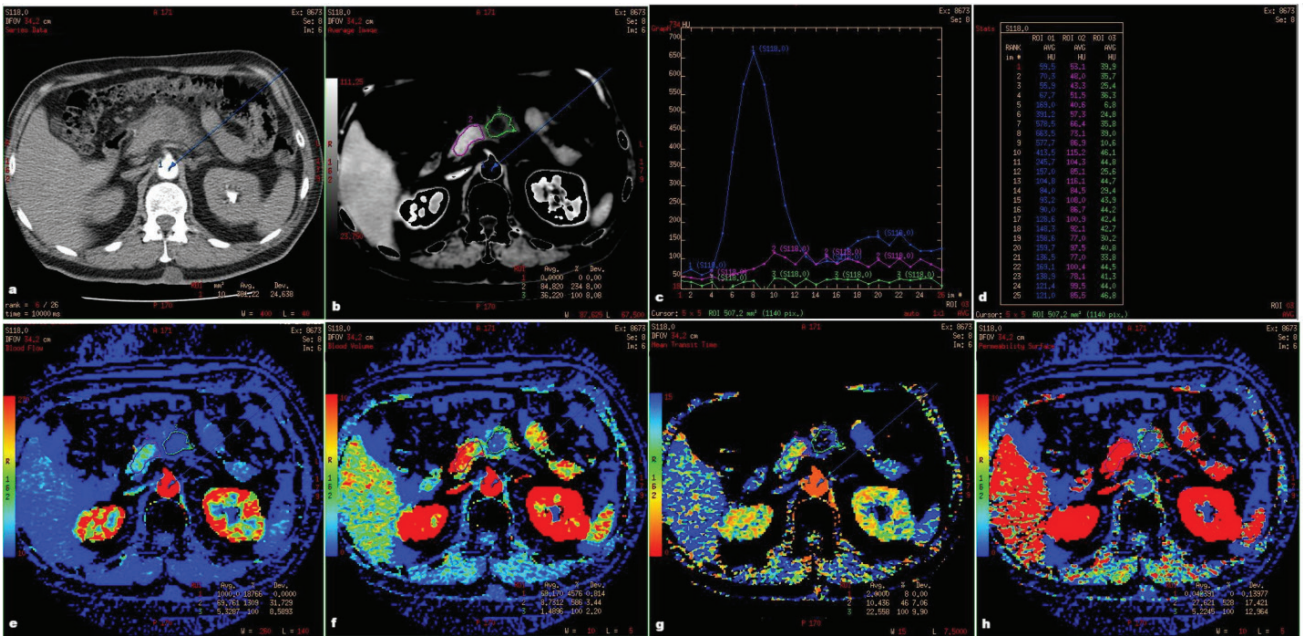

Figure 1. Analysis of the CT perfusion study: **a)** A CT image of the suspected tumor in the body of the pancreas and dot ROI in the abdominal aorta (blue) **b)** The reference image of the corresponding cross section of the CT perfusion study with the freehand ROIs in the tumor (green) and surrounding healthy pancreatic tissue (violet) **c)** The arterial, tumor and healthy pancreatic tissue time-density curve **d)** The table view of the arterial, tumor and healthy pancreatic tissue time-density curve **e)** BF **f)** BV **g)** MTT **e)** PS (Images are author's work and written informed consent for publishing their anonymous images was obtained from a patient)

Blood flow extraction product (EF, K trans): rate of one-way capillary diffusion of contrast medium from intravascular to extravascular space [ml/min/100ml] (Patlak's kinetic model).

Kinetic and mathematical models

The arterial, tumor, and healthy tissue time-density curves precisely show the change in density, i.e., the time dynamics of post-contrast attenuation in the artery and selected tissues (ROI) **(Figure 1a)**. Thus, the formation of the time-density curves is always the first step in the analysis of a CT perfusion study, regardless of the kinetic model used in subsequent analysis. The three basic postulates of CT perfusion are that 1) the concentration of iodine inside the blood vessels and tissues is linearly proportional to the resulting increase in attenuation, so the change in attenuation per unit of time can be analyzed using standard kinetic models by pixel-by-pixel calculations and displayed with color perfusion maps, 2) the contrast agent is distributed into intra-vascular and extravascular compartments, which gives rise to the possibility of calculating different physiological parameters that can be measured, and 3) the pharmacokinetic distribution of the contrast in two compartments (intra-vascular and extravascular) determines the aspects of vascular physiology that can be assessed by DCE-CT (1-4). Based on these postulates, three kinetic models are constructed to approximate tissue perfusion physiology and used in commercially available CT perfusion software.

Single-(One)-compartmental model (Maximum slope, Fick Principle): is the simplest kinetic model that takes into account only the intravascular compartment and the so-called "perfusion phase" that lasts for a time interval of about 45 s from the beginning of the contrast injection. It is based on Fick's principle, which approximates that the intravascular and extravascular spaces represent a single compartment (1-4). This is reliable only during the first pass of the contrast through the arterial and capillary blood vessels of the tissue, i.e., before the appearance of contrast in venous blood vessels. Since this kinetic model is limited to the "first pass" of the contrast through the arterial and capillary circulations, it enables quantification of only three tissue perfusion parameters: BF, BV, and MTT. BF is calculated according to the formula: maximum slope of tissue enhancement divided by peak arterial enhancement (1-4). For a correct assessment of perfusion using this model, the peak arterial enhancement must precede the peak tissue enhancement in time, as confirmed on the arterial-tissue time-density curve. This prerequisite is achieved by injecting a small amount of iodine contrast at a high speed (45-50 ml of contrast, flow 5-7 ml/s).

Two-compartmental model: calculates the BF value using the Maximum slope method. However, BV and K trans are calculated by using Patlak's (two-compartment) model (1-4). This kinetic model implies the existence of two separate compartments: intravascular and extravascular (extracellular, i.e., interstitial space), and is based on the assumption that the contrast moves exclusively in one direction: from the intravascular to the extravascular space (1-4). The return flux of contrast from the interstitial to the venous system is ignored in this kinetic model. K trans, as an indicator of capillary permeability in Patlak's kinetic model, represents the rate of one-way capillary diffusion of contrast from the intravascular to the extravascular space (1-4). For the calculation of K trans in this kinetic model, after the perfusion phase (0-45 s, at short scanning intervals of 1-2 s), an additional scanning lasting 15-30 s, in longer time intervals of up to 5 seconds, is recommended, which adds another 3-6 perfusion series (1).

Deconvolution model (Johnson-Wilson model, Distributed parameter model with adiabatic approximation of tissue homogeneity): takes into account the change in the contrast concentration gradient in the intra-vascular space (capillaries) for calculation the BF, BV and MTT as it assumes that the contrast concentration decreases linearly on the way from the "arterial inlet" to the "venous outlet" (1-4). PS is calculated by extending the deconvolution model, using the so-called "distributed parameter model", which considers the return flux of contrast medium from the interstitial space to the capillaries (1-4). Thus, capillary permeability surface area product (PS) in this kinetic model represents the ratio of volume of contrast that diffuse through the capillary endothelial membrane and the total surface area of the capillary wall, taking into account two-way diffusion: extravasation from the capillaries into the interstitial space and "return" of a part of the contrast from the interstitial space to the capillaries. For reliable calculation of PS in this kinetic model, after the perfusion phase (0-45 s, at intervals of 1-2 s), an additional scanning lasting 90 s (interstitial phase) is recommended, in less frequent time intervals, typically every 10-15 s, which adds another 6-9 perfusion series (1).

Concordance in quantitative perfusion parameters derived from multiple kinetic models and software

Significantly lower values of BF and higher values of BV for the same types of cancer can be obtained by applying the Maximum slope CT perfusion algorithm, compared to the algorithm based on the deconvolution kinetic model (16, 18-20). Different values of perfusion parameters for the same tumor can be obtained using different versions of the same commercially available CT perfusion software, for example, GE Perfusion version 3.0 and 4.0 (17) **(Figure 2a-h)**.

The most reliable CT perfusion algorithm might be assessed by comparing CT perfusion with direct measurement of oxygenation using a microprobe placed in the tissue of interest (21).

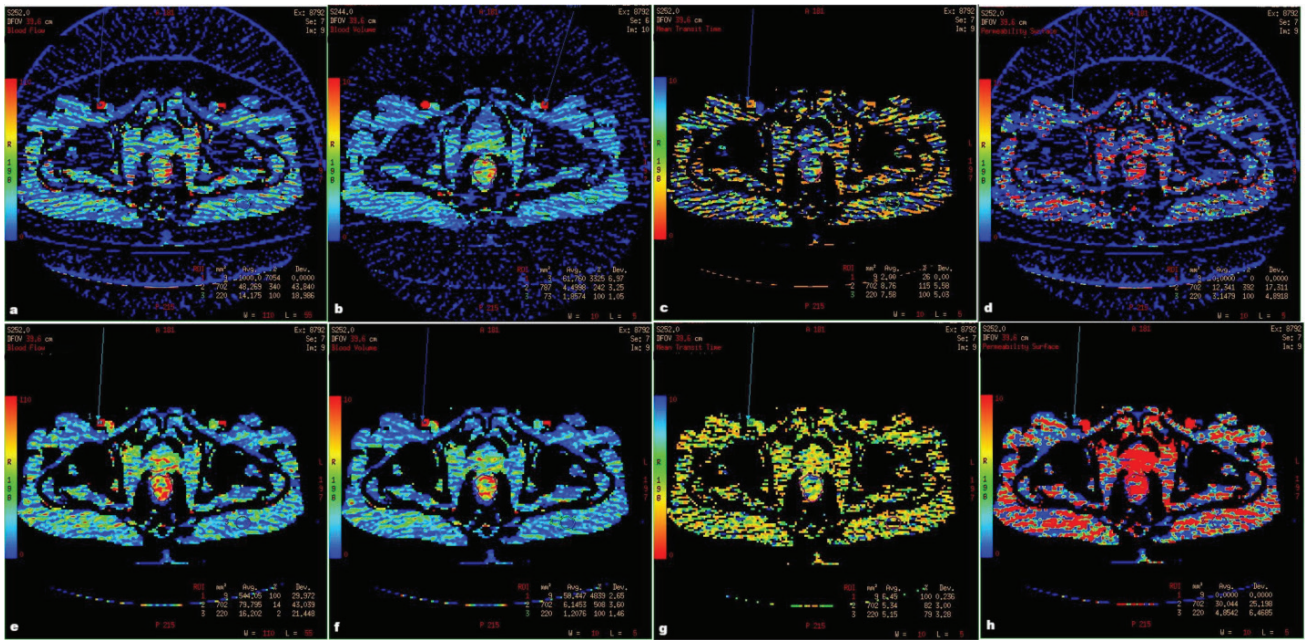

Figure 2. CT perfusion parameter values (BF, BV, MTT and PS) of the same tumor of the rectum (adenocarcinoma) after the neoadjuvant chemo-radiotherapy (violet) and neighboring skeletal muscle (green), obtained by two versions of the deconvolution- based commercial CT perfusion software: **(a-d)** GE Perfusion 3.0 **(e-h)** GE Perfusion 4.0 (Images are author's work and written informed consent for publishing their anonymous images was obtained from a patient)

To address inconsistencies in quantitative perfusion parameter values calculated with different CT perfusion software, Miles and colleagues proposed calculating the standardized perfusion value (SPV) (22). SPV represents a universal semi-quantitative indicator of tissue perfusion, proposed to simplify and unify CT perfusion measurements and enable comparison of perfusion and metabolism in tumors (22-26). Calculation of SPV, which represents tissue perfusion normalized to whole-body perfusion, was performed using the standardized uptake value (SUV) of 18-FDG, a widely used nuclear medicine metric (23). SPV, like SUV, is calculated according to a formula that considers only the peak tissue enhancement (PTE) from the time-density curve of a CT perfusion series **(Figure 1c-d)** and the patient's body mass (22, 26). The value of the constant, which is also included in the formula, depends on the tube voltage, volume, and iodine contrast concentration used (22, 26). The SPVs of lung, colorectal, breast, and esophageal cancer were reported in the literature (22-26). The SPV of esophageal carcinoma was significantly higher than that of skeletal muscle, which served as a control (26). The same was demonstrated for quantitative CT perfusion measurements, which proves the validity of SPV in discriminating between neoplastic and healthy tissue (22-26). Similarly, since it was reported that the CT perfusion parameter values positively correlated with the tumor MVD (27), the same may be assumed for the SPV. A cut-off value of SPV of 2.5 discriminates esophageal neoplasm from healthy muscular tissue with superior accuracy (26), which corresponds with the same cut-off value of SUV that is commonly used to distinguish malignant from benign lesions (25). Available reports also present that the SPVs of esophageal carcinoma and lung carcinoma are comparable (22, 23, 26). In brief, the SPV is a promising semi-quantitative indicator of tissue perfusion, independent of CT perfusion software, and can be easily calculated in everyday practice from the data in the time-density curve.

Spectrum of application of the CT perfusion in cancers

The goal of CT perfusion in cancer imaging is to display and quantify tumor vascularization using the spectrum of available perfusion parameters. Pathological vascularization of malignant tumors is based on neo-angiogenesis (28-30). Neo-angiogenesis plays a significant role in the growth and metastasis of malignant tumors, as well as in the response of malignant tumors to therapy (29). Histopathological analysis of the tumor, however, primarily focuses on the histological structure of the malignant tumor itself rather than its vascularization. A more detailed analysis of the tumor vasculature was made possible by immunohistochemical labeling of endothelial cells with monoclonal antibodies against CD31, CD34, or factor VIII (27). This enables counting, i.e., assessing the density of blood vessels whose endothelial cells have previously been immunohistochemically marked, within a given (micro)volume of the tumor: micro vessel density (MVD) (27, 31). Histological evaluation of MVD is therefore limited to only a few biopsy samples or surgical specimens, in which blood vessels within the tumor are counted at high magnification in the so-called hot-spot zones of densest (neo)vascularization (27, 31). However, the use of CT perfusion on modern MDCT devices enables visualization and quantification of the perfusion of the entire tumor.

Difference in perfusion parameters of malignant tumors and healthy tissue

Compared with the reference healthy tissue, the values of BF, BV, and PS are significantly higher, and MTT is shorter in malignant tumors (26, 33-35). Reference healthy tissue can represent a healthy part of the organ from which the tumor originates (the wall of the esophagus, stomach, rectum above or below the level of the tumor, lymph nodes, or the parenchymal organs such as liver, pancreas, kidneys) **(Figure 1)** (26, 32, 35). Alternatively, adjacent skeletal muscle was used as a reference healthy tissue sample (26, 33). The values of BF, BV, and PS are significantly higher. MTT is shorter in the tissue of hypopharyngeal, esophageal, stomach, and rectal cancer compared to the tissue of the adjacent skeletal muscle, which reflects the morphological and functional differences of the pathological, i.e., neo-vascularization and vascularization of healthy tissue (26, 33, 35) **(Figures 2-5)**. In neoplastic tissue, the vascular network is on average denser than in healthy tissue (30-32). Blood vessels are chaotically distributed and of uneven density, tortuous, fragile, and hyper-permeable (due to the presence of inter-endothelial cavities and intracellular pores, interrupted basement membrane, and absence of smooth muscle cells and pericytes in the wall). Arterio-venous (AV) shunts are frequent. Some blood vessels are blindly closed (30, 31, 38, 39). Due to the haphazard structure and architecture of the neo-vasculature, blood flow is uneven, from accelerated through AV shunts, slowed through tortuous blood vessels, and absent or reversed in blind or collapsed blood vessels, as reflected by the marked heterogeneity of the tumor on CT perfusion (**Figure 3a-h**). The collapse of newly formed blood vessels in the neoplasm is caused by increased pressure in the interstitial space due to the transfer of macromolecules and blood elements from the intravascular to the intercellular space through the hyperpermeable wall of blood vessels (39). This causes regional hypoxia within the tumor, despite a denser vascular network (on average, a higher MVD than in healthy tissue) (31, 39). In contrast, in healthy tissue, blood vessels are of uniform density and diameter, regularly distributed in a specific pattern that is repeated throughout the organ (30).

How do the structural and functional characteristics of neo-angiogenesis reflect on the quantitative value of CT perfusion parameters? The density, course, and width of the opened-lumen blood vessels determine blood flow, i.e., perfusion. BF is therefore considered the main indicator of tissue oxygenation (1-4, 39). Blood volume (total volume of circulating blood in blood vessels) is determined primarily by the density of blood vessels in the tissue (1-4, 39). Several studies have shown a significant correlation between MVD and CT perfusion parameters of various malignant tumors, primarily BV (27, 39-42).

In contrast, two studies related to adenocarcinoma of the stomach and colon found no correlation between BF and MVD (38, 40). Permeability surface area product primarily depends on the permeability of the vascular wall, as well as on the total volume (density) of blood vessels in the tissue (1-4, 29). Mean transit time is determined by the shape and width of the lumen of the blood vessels, as well as the pressure in the interstitial space (1-4, 29). In most types of neoplasms, all perfusion parameters, except MTT, are, on average, significantly higher than in reference healthy tissue (1-4, 29). One exception is pancreatic tissue, in which higher perfusion parameter values were measured compared with pancreatic adenocarcinoma

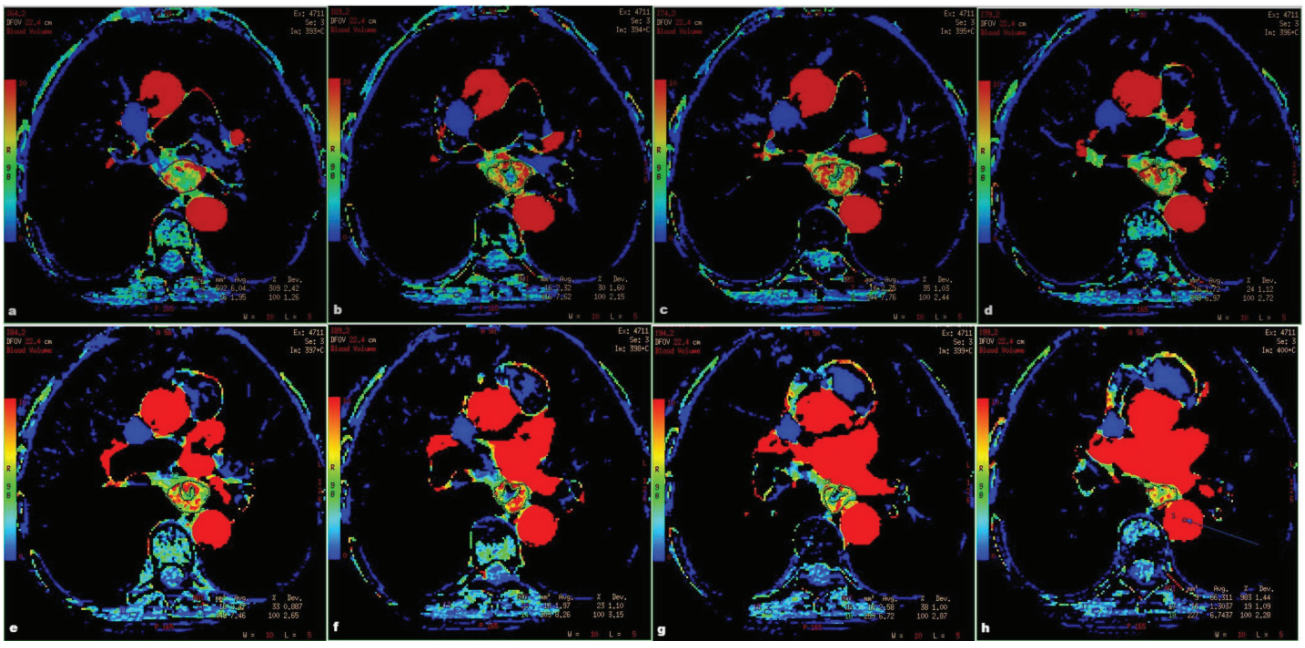

Figure 3. Perfusion heterogeneity in the same tumor (esophageal SCC) presented by the CT perfusion study: **(a-h)** BV of esophageal carcinoma and neighboring skeletal muscle on eight consecutive 5 mm-thick cross-sectional images (Images are the author's work, and written informed consent for publishing their anonymous images was obtained from the patient)

(Figure 1e-h) (43-45). This discrepancy may be related to the rich vascularization of the pancreatic tissue itself and to the pronounced desmoplastic reaction, i.e., intratumoral fibrosis, in pancreatic adenocarcinoma. Thus, intratumoral blood vessels are compressed by fibrosis, which explains the lower values of BF, BV, and PS in this, the most common malignant tumor of the pancreas, compared with the surrounding healthy pancreatic tissue **(Figure 1e-h)** (43-45).

Differentiation of malignant from benign tumors

In a large number of studies, it has been shown that malignant tumors and benign lesions of the same organ differ in CT perfusion parameters, allowing their non-invasive discrimination (36, 48-52). In parotid tumors, it has been reported that malignant tumors have significantly higher BF, BV, and PS than benign tumors (36). For lung nodules, which are a very frequent finding and a diagnostic challenge in everyday radiological practice, significantly higher BF and PS values for lung cancer compared to benign lung nodules have been reported, allowing reliable differentiation of these lesions (48, 49). Similar results were obtained for differentiating RCC from lipid-poor renal angiomyolipoma based on differences in CT perfusion parameters BV, BF, and PS (50). It is also possible to differentiate metastatic from intact cervical lymph nodes in patients with cancer of the larynx and hypopharynx based on significantly higher values of BF, BV, and PS (51), as well as in patients with cancer of the oral cavity based on a significantly shorter MTT in metastatic lymph nodes (52).

Non-invasive assessment of the degree of differentiation of neoplasms

Another role of CT perfusion in oncological imaging is the possibility of non-invasive differentiation of highly aggressive high-grade i.e. poorly differentiated, from low-grade i.e. well-differentiated neoplasms based on CT perfusion parameter values, which has been shown for different types of malignant tumors: gastric cancer (42), rectal cancer (53), pancreatic adenocarcinoma (45, 54-56), hepatocellular carcinoma (57), renal cell carcinoma (46), neuroendocrine neoplasm (58) and gastrointestinal stromal tumor (59). For all the aforementioned malignant tumors, except pancreatic adenocarcinoma, it was shown that higher values of perfusion parameters, except MTT, were quantified in poorly differentiated i.e., high-grade tumors compared to well-differentiated ones, which is a consequence of more extensive neo-vascularization in poorly differentiated, fast-growing neoplastic tissue (42, 46, 53, 57-59). Poorly differentiated adenocarcinomas of the pancreas had instead lower BF, BV, and PS values than moderately and well differentiated ones, which is explained by the compression of intratumoral blood vessels by the reach intratumoral fibrosis, which is characteristic of all carcinomas of biliopancreatic origin, and is more pronounced in poorly differentiated tumors (45, 54-56).

Assessment and monitoring of the response to neoadjuvant therapy based on CT perfusion

The value of CT perfusion in evaluating the response to neoadjuvant chemo-radiotherapy (nCRT) has been demonstrated in squamous cell carcinoma (SCC) of the esophagus (60-64). BF, BV, and PS values, quantified after nCRT, were significantly lower, and MTT was significantly longer, in patients with histologically proven complete response (pCR) compared with those with partial response (pPR) (60, 61). Significant differences in the values of perfusion parameters after nCRT in relation to histologically proved tumor regression grade (TRG) were also shown **(Figure 4a-f)** (60). These results indicate that the reduction in CT perfusion parameters after nCRT reflects the absence of pathological vascularization in the fibrous esophageal wall, where viable tumor tissue is no longer present (pCR). To test this assumption, future histological studies focused on changes in the vascular network after nCRT are needed; such studies are currently lacking. By comparing the basic post-contrast CT with the corresponding CT perfusion images section-by-section and in correlation with the histopathology findings, it was noted that the hyper-dense foci in the esophageal wall, which exactly match with the hyper-perfusion zones, in fact represent the residual viable neoplastic tissue after the nCRT **(Figure 4c-f)** (62).

Similar to esophageal SCC **(Figure 5a-h)**, studies of advanced head and neck SCC also showed that BF and BV values significantly decreased after definitive concomitant CRT in patients who responded to therapy (65).

Similar results have been shown in studies of gastric adenocarcinoma (66-68). BF, BV, and size reduction rate after three series of chemotherapy were significantly correlated with the pathological tumor regression grade (67). A decrease in PS after the 1st cycle of chemotherapy was an early predictor of a good clinical and pathological response to nCRT in gastroesophageal junction adenocarcinoma (66). Significant reductions in BF, BV, and PS were observed after concomitant CRT in patients with locally advanced gastric adenocarcinoma who had a good therapeutic response and longer survival (68).

The diagnostic and prognostic value of CT perfusion parameters was analyzed in patients with advanced non-small cell lung cancer (NSCLC) after chemotherapy, and it was shown that lower post-chemotherapy BV and PS predicted remission and longer survival (69). Similarly, all perfusion parameters (BF, BV, and PS) showed a consistent decrease during the early and late phases of anti-angiogenic therapy in advanced NSCLC in a pilot study by Aya et al. (70).

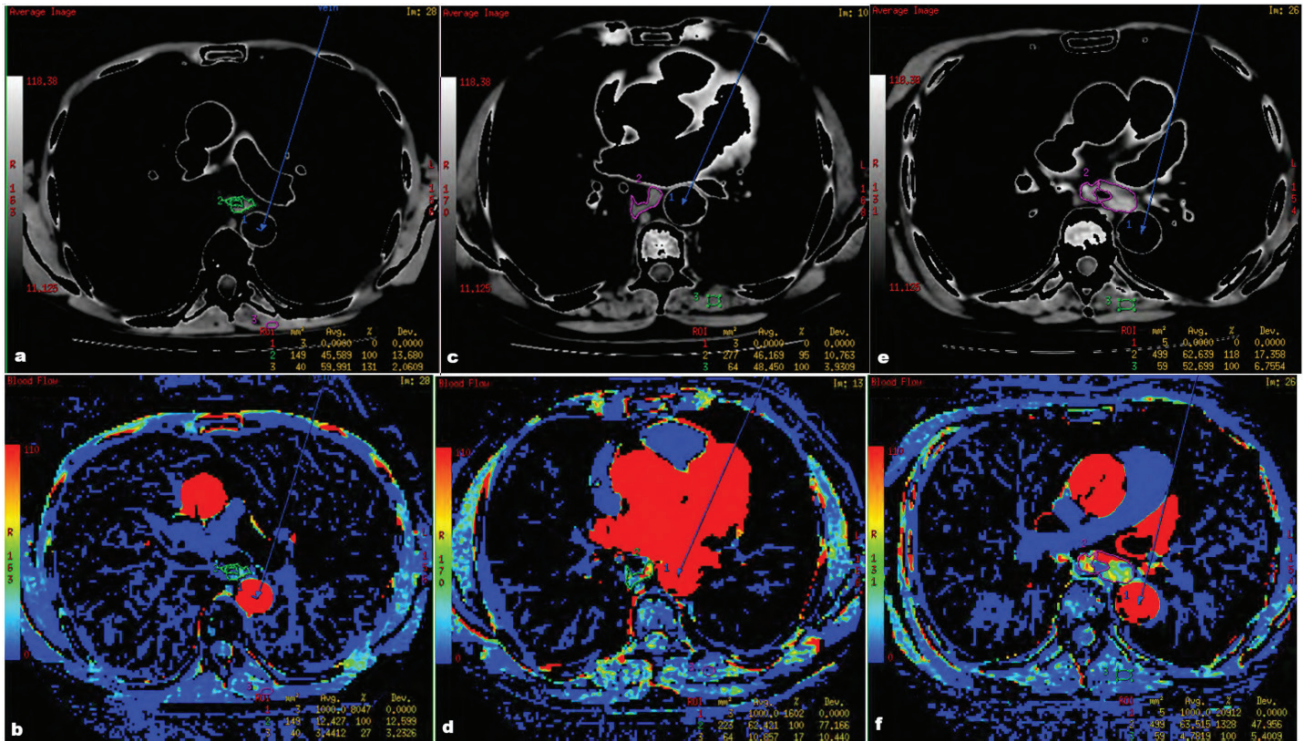

Figure 4. Differences in the values of CT perfusion parameter (BF) of the esophageal SCC after the neoadjuvant CRT in relation to histologically proved tumor regression grade (TRG): **(a-b)** TRG 1 (complete regression), **(c-d)** TRG 2 (strong partial regression), and **(e-f)** TRG 3 (moderate partial regression). (Images are the author's work, and written informed consent for publishing their anonymous images was obtained from patients)

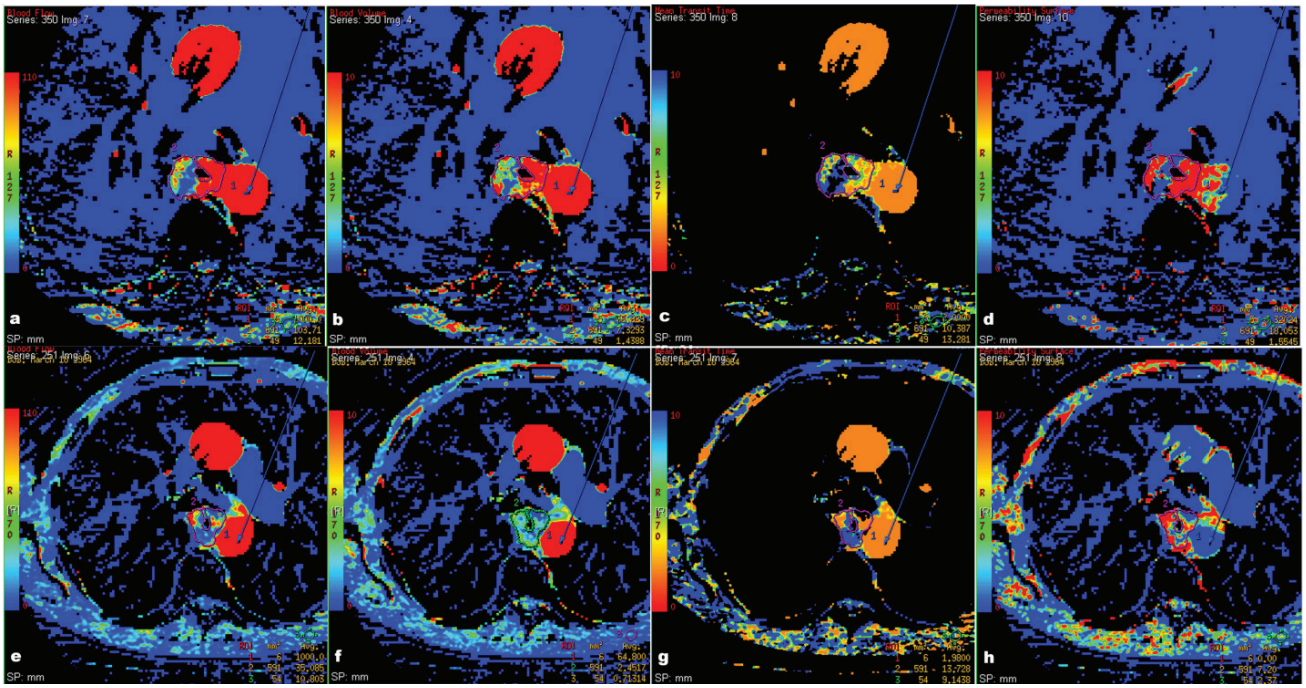

Figure 5. CT perfusion parameter values (BF, BV, MTT, and PS) of the esophageal SCC: **(a-d)** before and **(e-h)** after the neoadjuvant CRT (Images are the author's work, and written informed consent for publishing their anonymous images was obtained from a patient)

In studies related to rectal cancer, significant decreases in the perfusion parameters BF, BV, and PS and an increase in MTT after CRT were observed (35, 38, 71).

A significant decrease in all perfusion parameters, except MTT, was also observed in metastatic GIST that responded well to tyrosine-kinase inhibitor molecular therapy (72).

In the systematic review by Garbino et al., several studies were presented that assessed the therapeutic response of primary and secondary liver tumors to minimally invasive treatments, including TACE, chemotherapy, and biological therapy, using CT perfusion (5). In the majority of those studies, the value of CT perfusion in response assessment was demonstrated, with declines in

CT perfusion parameter values as a marker of satisfactory response and longer survival (5, 73, 74).

Unlike the majority of malignant tumors, in pancreatic adenocarcinoma, an increase in BF value after neoadjuvant CRT was a reliable indicator of a good histological response, as shown in the study by Hamdi and coauthors (75).

Radiation dose

A main disadvantage of CT perfusion is the additional radiation dose to the patient. In the guidelines for performing CT perfusion of the Experimental Cancer Medicine Center Imaging Network Group, it was recommended that the maximum effective dose of 20 mSv, or 30 mSv for volumes larger than 4 cm in the Z-axis, should not be exceeded (1). Low-dose CT perfusion techniques by using the 80 kV or 100 kV tube voltage and low tube current (30-100 mAs) could be done with much lower effective doses of radiation (Table 1), even if large volume coverage (up to 16 cm) was achieved by using the 256-640-detector rows scanners (76-78). However, some novel CT techniques, such as dual-energy CT, may replace perfusion CT with similar information on tissue perfusion and lower radiation exposure (79, 80).

CONCLUSION

In conclusion, CT perfusion allows potential non-invasive discrimination of the neoplasm from healthy tissue, malignant from benign tumors, highly aggressive from low aggressive tumors, and good from poor response to oncologic treatment. CT perfusion introduces elements of functional diagnostics into morphological imaging of tumors, while low-dose scanning protocols enable its safe incorporation into everyday radiological practice for oncology patients. The lack of standardization of CT perfusion protocols and the lack of interchangeability of results across different CT systems and centers are among the main limitations in fully achieving this aim.

Acknowledgement: N/A

Funding Information: The Ministry of Science, Technological Development and Innovation of Republic of Serbia has supported this work through a Grant Agreement with the University of Belgrade, Faculty of Medicine No: 451-03-137/2025-03/ 200110

Conflicts of interest: The authors have no conflicts of interest to report.

Author contributions: Conceptualization: A.Đ-S., Methodology: M.MJ, J.K, A.I., Resources: S.O, N.G, D.S, P.S.,Writing – Original Draft Preparation: A.Đ-S., Writing – Review & Editing: M.MJ, J.K, A.I, S.O, N.G, D.S, P.S.

Ethical approval: N/A

Informed consent: N/A

References

1. Miles KA, Lee TY, Goh V, Klotz E, Cuenod C, Bisdas S, et al. Current status and guidelines for the assessment of tumour vascular support with dynamic contrast-enhanced computed tomography. Eur Radiol. 2012; 22: 1430-41. doi: 10.1007/s00330-012-2379-4.
2. Zeng D, Zeng C, Zeng Z, Li S, Deng Z, Chen S, et al. Basis and current state of computed tomography perfusion imaging: a review. Phys Med Biol. 2022; 67(18). doi: 10.1088/1361-6560/ac8717.
3. Bellomi M, Viotti S, Preda L, D'Andrea G, Bonello L, Petralia G. Perfusion CT in solid body-tumours. Part II: Clinical applications and future development. Radiol Med. 2010; 115: 858-74. doi: 10.1007/s11547-010-0545-9.
4. Petralia G, Preda L, D'Andrea G, Viotti S, Bonello L, De Filippi R, Bellomi M. CT perfusion in solid-body tumours. Part I: Technical issues. Radiol Med. 2010; 115: 843-57. doi: 10.1007/s11547-010-0519-y.
5. Garbino N, Brancato V, Salvatore M, Cavaliere C. A Systematic Review on the Role of the Perfusion Computed Tomography in Abdominal Cancer. Dose Response. 2021; 19: 15593258211056199. doi: 10.1177/15593258211056199.
6. Tian C, Chen J, Zhang J, Du F. Assessment of cerebral hemodynamic changes in acute ischemic stroke patients following mechanical thrombectomy using CT perfusion imaging. Front Neurol. 2025; 16: 1628717. doi: 10.3389/fneur.2025.
7. Broocks G, McDonough RV, Bechstein M, Klapproth S, Faizy TD, Schön G, et al. Thrombectomy in Patients with Ischemic Stroke Without Salvageable Tissue on CT Perfusion. Stroke. 2024; 55: 1317-25. doi: 10.1161/STROKEAHA.123.044916.
8. Georgievski-Brkic B, Savic M, Nikolic D, Nikcevic L, Vukicevic M, Kozic D. Evaluation of functional outcome measured by modified Rankin scale in rtPA treated patients with acute ischemic stroke. Arch Ital Biol. 2016; 154: 125-32. doi: 10.12871/00039829201643.
9. Kawaguchi Y, Kato S, Horita N, Utsunomiya D. Value of dynamic computed tomography myocardial perfusion in CAD: a systematic review and meta-analysis. Eur Heart J Cardiovasc Imaging. 2024; 25: 1675-85. doi: 10.1093/ehjci/jeae118.
10. Michallek F, Nakamura S, Takafuji M, Nagasawa N, Kurita T, Dohi K, et al. Fractal analysis of dynamic stress myocardial CT perfusion decouples diagnostic accuracy for obstructive coronary artery disease from remote flow. Jpn J Radiol. 2025 Oct 8. doi: 10.1007/s11604-025-01883-6.
11. Agarwal R, Agarwal MK, Gupta U, Gupta A. Early perfusion computed tomography in severe acute pancreatitis: Predicting necrosis and guiding care. Int J Crit Illn Inj Sci. 2025; 15: 82-89. doi: 10.4103/ijciis.ijciis_9_25.
12. Nozawa S, Kuwatani M, Shimura R, Sugiura R, Kawakubo K, Nagai K, et al. Efficacy of Perfusion Computed Tomography in Early Prediction of Post-endoscopic Retrograde Cholangiopancreatography Pancreatitis. Pancreas. 2025 Sep 18. doi: 10.1097/MPA.0000000000002568.
13. Axel L. Cerebral blood flow determination by rapid-sequence computed tomography: theoretical analysis. Radiology. 1980; 137: 679-86. doi: 10.1148/radiology.137.3.7003648.
14. Axel L. Tissue mean transit time from dynamic computed tomography by a simple deconvolution technique. Invest Radiol. 1983; 18: 94-9. doi: 10.1097/00004424-198301000-00018.
15. Miles KA, Hayball MP, Dixon AK. Functional images of hepatic perfusion obtained with dynamic CT. Radiology. 1993; 188: 405-11. doi: 10.1148/radiology.188.2.8327686.
16. Djuric-Stefanovic A, Saranovic Dj, Masulovic D, Ivanovic A, Pesko P. Comparison between the deconvolution and maximum slope 64-MDCT perfusion analysis of the esophageal cancer: is con-

version possible? Eur J Radiol. 2013; 82: 1716-23. doi: 10.1016/j.ejrad.2013.05.038.

17. Goh V, Halligan S, Bartram CI. Quantitative tumor perfusion assessment with multidetector CT: are measurements from two commercial software packages interchangeable? Radiology. 2007; 242: 777-82. doi: 10.1148/radiol.2423060279.
18. Bisdas S, Konstantinou G, Surlan-Popovic K, Khoshneviszadeh A, Baghi M, Vogl TJ, et al. Dynamic contrast-enhanced CT of head and neck tumors: comparison of first-pass and permeability perfusion measurements using two different commercially available tracer kinetics models. Acad Radiol. 2008; 15: 1580-9. doi: 10.1016/j.acra.2008.05.021.
19. Deniffel D, Boutelier T, Labani A, Ohana M, Pfeiffer D, Roy C. Computed Tomography Perfusion Measurements in Renal Lesions Obtained by Bayesian Estimation, Advanced Singular-Value Decomposition Deconvolution, Maximum Slope, and Patlak Models: Intermodel Agreement and Diagnostic Accuracy of Tumor Classification. Invest Radiol. 2018; 53: 477-85. doi: 10.1097/RLI.0000000000000477.
20. Koell M, Klauss M, Skornitzke S, Mayer P, Fritz F, Stiller W, et al. Computed Tomography Perfusion Analysis of Pancreatic Adenocarcinoma using Deconvolution, Maximum Slope, and Patlak Methods - Evaluation of Diagnostic Accuracy and Interchangeability of Cut-Off Values. Rofo. 2021; 193: 1062-73. English. doi: 10.1055/a-1401-0333.
21. Hemphill JC 3rd, Smith WS, Sonne DC, Morabito D, Manley GT. Relationship between brain tissue oxygen tension and CT perfusion: feasibility and initial results. AJNR Am J Neuroradiol. 2005; 26:1095-100. PMID: 15891166; PMCID: PMC8158594.
22. Miles KA, Griffiths MR, Fuentes MA. Standardized perfusion value: universal CT contrast enhancement scale that correlates with FDG PET in lung nodules. Radiology. 2001; 220: 548-53. doi: 10.1148/radiology.220.2.r01au26548.
23. Shastry M, Miles KA, Win T, Janes SM, Endozo R, Meagher M, et al. Integrated 18F-fluorodeoxyglucose-positron emission tomography/dynamic contrast-enhanced computed tomography to phenotype non-small cell lung carcinoma. Mol Imaging. 2012; 11: 353-60. PMID: 22954179; PMCID: PMC4210517.
24. Groves AM, Wishart GC, Shastry M, Moyle P, Iddles S, Britton P, et al. Metabolic-flow relationships in primary breast cancer: feasibility of combined PET/dynamic contrast-enhanced CT. Eur J Nucl Med Mol Imaging. 2009; 36: 416-21. doi: 10.1007/s00259-008-0948-1.
25. Sauter AW, Winterstein S, Spira D, Hetzel J, Schulze M, Mueller M, et al. Multifunctional profiling of non-small cell lung cancer using 18F-FDG PET/CT and volume perfusion CT. J Nucl Med. 2012; 53: 521-9. doi: 10.2967/jnumed.111.097865.
26. Djuric-Stefanovic A, Saranovic D, Sobic-Saranovic D, Masulovic D, Artiko V. Standardized perfusion value of the esophageal carcinoma and its correlation with quantitative CT perfusion parameter values. Eur J Radiol. 2015; 84: 350-359. doi: 10.1016/j.ejrad.2014.12.004.
27. Chen TW, Yang ZG, Wang QL, Li Y, Qian LL, Chen HJ. Whole tumour quantitative measurement of first-pass perfusion of oesophageal squamous cell carcinoma using 64-row multidetector computed tomography: correlation with microvessel density. Eur J Radiol. 2011; 79: 218-23. doi: 10.1016/j.ejrad.2010.03.024.
28. Folkman J. Tumor angiogenesis: therapeutic implications. N Engl J Med. 1971; 285: 1182-6. doi: 10.1056/NEJM197111182852108.
29. Cuenod CA, Fournier L, Balvay D, Guinebretière JM. Tumor angiogenesis: pathophysiology and implications for contrast-enhanced MRI and CT assessment. Abdom Imaging. 2006; 31: 188-93. doi: 10.1007/s00261-005-0386-5.
30. Konerding MA, Fait E, Gaumann A. 3D microvascular architecture of pre-cancerous lesions and invasive carcinomas of the colon. Br J Cancer. 2001; 84: 1354-62. doi: 10.1054/bjoc.2001.1809.
31. Bossi P, Viale G, Lee AK, Alfano R, Coggi G, Bosari S. Angiogenesis in colorectal tumors: microvessel quantitation in adenomas and carcinomas with clinicopathological correlations. Cancer Res. 1995; 55: 5049-53. PMID: 7585550.
32. Goh V, Halligan S, Taylor SA, Burling D, Bassett P, Bartram CI. Differentiation between diverticulitis and colorectal cancer: quantitative CT perfusion measurements versus morphologic criteria-initial experience. Radiology. 2007; 242: 456-62. doi: 10.1148/radiol.2422051670.
33. Goh V, Halligan S, Hugill JA, Bartram CI. Quantitative assessment of tissue perfusion using MDCT: comparison of colorectal cancer and skeletal muscle measurement reproducibility. AJR Am J Roentgenol. 2006; 187: 164-9. doi: 10.2214/AJR.05.0050.
34. Sahani DV, Holalkere NS, Mueller PR, Zhu AX. Advanced hepatocellular carcinoma: CT perfusion of liver and tumor tissue-initial experience. Radiology. 2007; 243: 736-43. doi: 10.1148/radiol.2433052020.
35. Bellomi M, Petralia G, Sonzogni A, Zampino MG, Rocca A. CT perfusion for the monitoring of neoadjuvant chemotherapy and radiation therapy in rectal carcinoma: initial experience. Radiology. 2007; 244: 486-93. doi: 10.1148/radiol.2442061189.
36. Niazi M, Mohammadzadeh M, Aghazadeh K, Sharifian H, Karimi E, Shakiba M, et al. Perfusion Computed Tomography Scan Imaging in Differentiation of Benign from Malignant Parotid Lesions. Int Arch Otorhinolaryngol. 2020; 24: e160-9. doi: 10.1055/s-0039-1697005.
37. Hashizume H, Baluk P, Morikawa S, McLean JW, Thurston G, Roberge S, Jain RK, McDonald DM. Openings between defective endothelial cells explain tumor vessel leakiness. Am J Pathol. 2000 Apr;156: 1363-80. doi: 10.1016/S0002-9440(10)65006-7.
38. Goh V, Padhani AR, Rasheed S. Functional imaging of colorectal cancer angiogenesis. Lancet Oncol. 2007; 8: 245-55. doi: 10.1016/S1470-2045(07)70075-X.
39. Song T, Shen YG, Jiao NN, Li XH, Hu HT, Qu JR, et al. Esophageal squamous cell carcinoma: assessing tumor angiogenesis using multislice CT perfusion imaging. Dig Dis Sci. 2012; 57: 2195-202. doi: 10.1007/s10620-012-2149-9.
40. Yao J, Yang ZG, Chen HJ, Chen TW, Huang J. Gastric adenocarcinoma: can perfusion CT help to noninvasively evaluate tumor angiogenesis? Abdom Imaging. 2011; 36: 15-21. doi: 10.1007/s00261-010-9609-5.
41. Li Y, Yang ZG, Chen TW, Chen HJ, Sun JY, Lu YR. Peripheral lung carcinoma: correlation of angiogenesis and first-pass perfusion parameters of 64-detector row CT. Lung Cancer. 2008; 61: 44-53. doi: 10.1016/j.lungcan.2007.10.021.
42. Satoh A, Shuto K, Okazumi S, Ohira G, Natsume T, Hayano K, et al. Role of perfusion CT in assessing tumor blood flow and malignancy level of gastric cancer. Dig Surg. 2010; 27: 253-60. doi: 10.1159/000288703.
43. Kandel S, Kloeters C, Meyer H, Hein P, Hilbig A, Rogalla P. Whole-organ perfusion of the pancreas using dynamic volume CT in patients with primary pancreas carcinoma: acquisition technique, post-processing and initial results. Eur Radiol. 2009; 19: 2641-6. doi: 10.1007/s00330-009-1453-z.
44. Yadav AK, Sharma R, Kandasamy D, Pradhan RK, Garg PK, Bhalla AS, et al. Perfusion CT - Can it resolve the pancreatic carcinoma versus mass forming chronic pancreatitis conundrum? Pancreatology. 2016; 16: 979-87. doi: 10.1016/j.pan.2016.08.011.
45. Kovač JD, Đurić-Stefanović A, Dugalić V, Lazić L, Stanisavljević D, Galun D, et al. CT perfusion and diffusion-weighted MR imaging of pancreatic adenocarcinoma: can we predict tumor grade using functional parameters? Acta Radiol. 2019; 60: 1065-73. doi: 10.1177/0284185118812202.
46. Chen C, Liu Q, Hao Q, Xu B, Ma C, Zhang H, et al. Study of 320-slice dynamic volume CT perfusion in different pathologic types of kidney tumor: preliminary results. PLoS One. 2014; 9: e85522. doi: 10.1371/journal.pone.0085522.
47. Yu C, Li T, Zhang R, Yang X, Yang Z, Xin L, et al. Dual-energy CT perfusion imaging for differentiating WHO subtypes of thymic epithelial tumors. Sci Rep. 2020; 10: 5511. doi: 10.1038/s41598-020-62466-1.
48. Huang C, Liang J, Lei X, Xu X, Xiao Z, Luo L. Diagnostic Performance of Perfusion Computed Tomography for Differentiating Lung Cancer from Benign Lesions: A Meta-Analysis. Med Sci Monit. 2019; 25: 3485-94. doi: 10.12659/MSM.914206.

49. Hu X, Gou J, Wang L, Lin W, Li W, Yang F. Diagnostic accuracy of low-dose dual-input computed tomography perfusion in the differential diagnosis of pulmonary benign and malignant ground-glass nodules. Sci Rep. 2024; 14: 17098. doi: 10.1038/s41598-024-68143-x.
50. Chen C, Kang Q, Xu B, Shi Z, Guo H, Wei Q, et al. Fat poor angiomyolipoma differentiation from renal cell carcinoma at 320-slice dynamic volume CT perfusion. Abdom Radiol (NY). 2018; 43: 1223-30. doi: 10.1007/s00261-017-1286-1.
51. Trojanowska A, Trojanowski P, Bisdas S, Staśkiewicz G, Drop A, Klatka J, et al. Squamous cell cancer of hypopharynx and larynx - evaluation of metastatic nodal disease based on computed tomography perfusion studies. Eur J Radiol. 2012; 81: 1034-9. doi: 10.1016/j.ejrad.2011.01.084.
52. Suryavanshi S, Kumar J, Manchanda A, Singh I, Khurana N. Comparison of CECT and CT perfusion in differentiating benign from malignant neck nodes in oral cavity cancers. Eur J Radiol Open. 2021; 8: 100339. doi: 10.1016/j.ejro.2021.100339.
53. Xu Y, Sun H, Song A, Yang Q, Lu X, Wang W. Predictive Significance of Tumor Grade Using 256-Slice CT Whole-Tumor Perfusion Imaging in Colorectal Adenocarcinoma. Acad Radiol. 2015; 22: 1529-35. doi: 10.1016/j.acra.2015.08.023.
54. D'Onofrio M, Gallotti A, Mantovani W, Crosara S, Manfrin E, Falconi M, et al. Perfusion CT can predict tumoral grading of pancreatic adenocarcinoma. Eur J Radiol. 2013; 82: 227-33. doi: 10.1016/j.ejrad.2012.09.023.
55. Perik TH, van Genugten EAJ, Aarntzen EHJG, Smit EJ, Huisman HJ, Hermans JJ. Quantitative CT perfusion imaging in patients with pancreatic cancer: a systematic review. Abdom Radiol (NY). 2022; 47: 3101-17. doi: 10.1007/s00261-021-03190-w.
56. Zaboriene I, Zviniene K, Lukosevicius S, Ignatavicius P, Barauskas G. Dynamic Perfusion Computed Tomography and Apparent Diffusion Coefficient as Potential Markers for Poorly Differentiated Pancreatic Adenocarcinoma. Dig Surg. 2021; 38: 128-35. doi: 10.1159/000511973.
57. Lewin M, Laurent-Bellue A, Desterke C, Radu A, Feghali JA, Farah J, et al. Evaluation of perfusion CT and dual-energy CT for predicting microvascular invasion of hepatocellular carcinoma. Abdom Radiol (NY). 2022; 47: 2115-27. doi: 10.1007/s00261-022-03511-7.
58. Notake T, Shimizu A, Kubota K, Sugenoya S, Umemura K, Goto T, et al. Usefulness of intratumoral perfusion analysis for assessing biological features of non-functional pancreatic neuroendocrine neoplasm. Langenbecks Arch Surg. 2024; 409: 38. doi: 10.1007/s00423-023-03219-2.
59. Mitrovic-Jovanovic M, Djuric-Stefanovic A, Ebrahimi K, Dakovic M, Kovac J, Šarac D, et al. The Utility of Conventional CT, CT Perfusion and Quantitative Diffusion-Weighted Imaging in Predicting the Risk Level of Gastrointestinal Stromal Tumors of the Stomach: A Prospective Comparison of Classical CT Features, CT Perfusion Values, Apparent Diffusion Coefficient and Intravoxel Incoherent Motion-Derived Parameters. Diagnostics (Basel). 2022; 12: 2841. doi: 10.3390/diagnostics12112841.
60. Djuric-Stefanovic A, Micev M, Stojanovic-Rundic S, Pesko P, Saranovic Dj. Absolute CT perfusion parameter values after the neoadjuvant chemoradiotherapy of the squamous cell esophageal carcinoma correlate with the histopathologic tumor regression grade. Eur J Radiol. 2015; 84: 2477-84. doi: 10.1016/j.ejrad.2015.09.025.
61. Djuric-Stefanovic A, Saranovic D, Micev M, Stankovic V, Plesinac-Karapandzic V, Pesko P, et al. Does the computed tomography perfusion imaging improve the diagnostic accuracy in the response evaluation of esophageal carcinoma to the neoadjuvant chemoradiotherapy? Preliminary study. J BUON. 2014; 19: 237-44. PMID: 24659670.
62. Djuric-Stefanovic A, Jankovic A, Saponjski D, Micev M, Stojanovic-Rundic S, Cosic-Micev M, Pesko P. Analyzing the post-contrast attenuation of the esophageal wall on routine contrast-enhanced MDCT examination can improve the diagnostic accuracy in response evaluation of the squamous cell esophageal carcinoma to neoadjuvant chemoradiotherapy in comparison with the esophageal wall thickness. Abdom Radiol (NY). 2019; 44: 1722-1733. doi: 10.1007/s00261-019-01911-w.
63. Hayano K, Okazumi S, Shuto K, Matsubara H, Shimada H, Nabeya Y, et al. Perfusion CT can predict the response to chemoradiation therapy and survival in esophageal squamous cell carcinoma: initial clinical results. Oncol Rep. 2007; 18: 901-8. PMID: 17786353.
64. Makari Y, Yasuda T, Doki Y, Miyata H, Fujiwara Y, Takiguchi S, et al. Correlation between tumor blood flow assessed by perfusion CT and effect of neoadjuvant therapy in advanced esophageal cancers. J Surg Oncol. 2007; 96: 220-9. doi: 10.1002/jso.20820.
65. Surlan-Popovic K, Bisdas S, Rumboldt Z, Koh TS, Strojan P. Changes in perfusion CT of advanced squamous cell carcinoma of the head and neck treated during the course of concomitant chemoradiotherapy. AJNR Am J Neuroradiol. 2010; 31: 570-5. doi: 10.3174/ajnr.A1859.
66. Lundsgaard Hansen M, Fallentin E, Lauridsen C, Law I, Federspiel B, Bæksgaard L, et al. Computed tomography (CT) perfusion as an early predictive marker for treatment response to neoadjuvant chemotherapy in gastroesophageal junction cancer and gastric cancer--a prospective study. PLoS One. 2014; 9: e97605. doi: 10.1371/journal.pone.0097605.
67. Sun Z, Cheng X, Ge Y, Shao L, Xuan Y, Yan G. An application study of low-dose computed tomography perfusion imaging for evaluation of the efficacy of neoadjuvant chemotherapy for advanced gastric adenocarcinoma. Gastric Cancer. 2018; 21: 413-420. doi: 10.1007/s10120-017-0763-0.
68. Liang JX, Bi XJ, Li XM, Gao ZL, Suo F, Cui EG, et al. Evaluation of Multislice Spiral Computed Tomography Perfusion Imaging for the Efficacy of Preoperative Concurrent Chemoradiotherapy in Middle-aged and Elderly Patients with Locally Advanced Gastric Cancer. Med Sci Monit. 2018; 24: 235-245. doi: 10.12659/msm.905143.
69. Lin G, Sui Y, Li Y, Huang W. Diagnostic and prognostic value of CT perfusion parameters in patients with advanced NSCLC after chemotherapy. Am J Transl Res. 2021; 13: 13516-23. PMID: 35035693.
70. Aya F, Benegas M, Viñolas N, Reyes R, Vollmer I, Arcocha A, et al. A Pilot Study to Evaluate Early Predictive Value of Thorax Perfusion-CT in Advanced NSCLC. Cancers (Basel). 2021; 13: 5566. doi: 10.3390/cancers13215566.
71. Curvo-Semedo L, Portilha MA, Ruivo C, Borrego M, Leite JS, Caseiro-Alves F. Usefulness of perfusion CT to assess response to neoadjuvant combined chemoradiotherapy in patients with locally advanced rectal cancer. Acad Radiol. 2012; 19: 203-13. doi: 10.1016/j.acra.2011.10.019.
72. Schlemmer M, Sourbron SP, Schinwald N, Nikolaou K, Becker CR, Reiser MF, et al. Perfusion patterns of metastatic gastrointestinal stromal tumor lesions under specific molecular therapy. Eur J Radiol. 2011; 77: 312-8. doi: 10.1016/j.ejrad.2009.07.031.
73. Ippolito D, Fior D, Bonaffini PA, Capraro C, Leni D, Corso R, et al. Quantitative evaluation of CT-perfusion map as indicator of tumor response to transarterial chemoembolization and radiofrequency ablation in HCC patients. Eur J Radiol. 2014; 83: 1665-71. doi: 10.1016/j.ejrad.2014.05.040.
74. Kalarakis G, Chryssou EG, Perisinakis K, Klontzas ME, Samonakis D, Hatzidakis A. CT perfusion and MRI: A combined approach for hepatocellular carcinoma diagnosis and follow-up after locoregional treatment. Eur J Radiol. 2025; 183: 111928. doi: 10.1016/j.ejrad.2025.
75. Hamdy A, Ichikawa Y, Toyomasu Y, Nagata M, Nagasawa N, Nomoto Y, et al. Perfusion CT to Assess Response to Neoadjuvant Chemotherapy and Radiation Therapy in Pancreatic Ductal Adenocarcinoma: Initial Experience. Radiology. 2019; 292: 628-35. doi: 10.1148/radiol.2019182561.
76. Li P, Deng W, Xue H, Xu K, Zhu L, Li J, et al. Weight-adapted ultra-low-dose pancreatic perfusion CT: radiation dose, image quality, and perfusion parameters. Abdom Radiol (NY). 2019; 44: 2196-204. doi: 10.1007/s00261-019-01938-z.
77. Konno Y, Hiraka T, Kanoto M, Sato T, Tsunoda M, Ishizawa T, et al. Pancreatic perfusion imaging method that reduces radiation dose and maintains image quality by combining volumetric perfusion CT with multiphasic contrast enhanced-CT. Pancreatology. 2020; 20: 1406-12. doi: 10.1016/j.pan.2020.08.010.

78. Marin D, Nelson RC, Barnhart H, Schindera ST, Ho LM, Jaffe TA, et al. Detection of pancreatic tumors, image quality, and radiation dose during the pancreatic parenchymal phase: effect of a low-tube-voltage, high-tube-current CT technique- preliminary results. Radiology. 2010; 256: 450-9. doi: 10.1148/radiol.10091819.

79. Gordic S, Puippe GD, Krauss B, Klotz E, Desbiolles L, Lesurtel M, et al. Correlation between Dual-Energy and Perfusion CT in Patients with Hepatocellular Carcinoma. Radiology. 2016; 280: 78-87. doi: 10.1148/radiol.2015151560.

80. Mulé S, Pigneur F, Quelever R, Tenenhaus A, Baranes L, Richard P, et al. Can dual-energy CT replace perfusion CT for the functional evaluation of advanced hepatocellular carcinoma? Eur Radiol. 2018; 28: 1977-85. doi: 10.1007/s00330-017-5151-y.

CT PERFUZIJA U ONKOLOŠKOM IMIDŽINGU

Aleksandra Đurić-Stefanović[1,2], Milica Mitrović Jovanović[1,2], Jelena Kovač[1,2], Aleksandar Ivanović[1,2], Slavenko Ostojić[1,3], Nikica Grubor[1,3], Dejan Stojakov[1,4], Predrag Sabljak[1,3]

Sažetak

CT perfuzija je metoda pregleda koja omogućava vizualizaciju i neinvazivnu kvantitativnu procenu perfuzije tkiva. Primena CT perfuzije u onkološkoj dijagnostici omogućava neinvazivno otkrivanje i kvantifikaciju neoangiogeneze (tj. patološke vaskularizacije) različitih malignih tumora. Na osnovu vrednosti parametara CT perfuzije moguće je razlikovati neoplazmu od zdravog tkiva, maligne od benignih tumora, visokoagresivne od niskoagresivnih tumora, kao i dobar od lošeg odgovora tumora na onkološku terapiju. Osnovni princip izvođenja niskodozne CT perfuzije podrazumeva ponovljeno skeniranje odabrane regije gde se nalazi tumor, uz redukciju napona i jačine struje u rendgenskoj cevi, u kratkim vremenskim intervalima nakon intravenske primene bolusa male količine jodnog kontrasta automatskim injektorom sa velikom brzinom protoka. Primenom različitih kinetičko-matematičkih modela moguće je meriti sledeće parametre perfuzije tkiva: protok krvi (BF), zapreminu cirkulišuće krvi (BV), srednje vreme prolaza kroz vaskularnu mrežu (MTT) i vaskularnu permeabilnost (PS ili K trans). Dok rezultati dobijeni različitim softverima za CT perfuziju nisu komparabilni, standardizovana perfuziona vrednost (SPV) je univerzalni semikvantitativni indikator perfuzije tkiva, koji je nezavistan od CT perfuzionog algoritma i može se jednostavno izračunati u odsustvu komercijalnog CT perfuzionog softvera. Dok su vrednosti BF, BV i PS značajno veće kod većine visokogradnih malignih tumora, u poređenju sa niskogradnim tumorima, kao i benignim tumorima ili zdravim tkivom, MTT je često kraće u visokogradusnim tumorima. Značajno smanjenje vrednosti CT perfuzionih parametara je znak dobrog odgovora neoplazme na onkološku terapiju.

Ključne reči: CT perfuzija, imidžing, onkologija, CT

Primljen: 01. 01. 2026. I **Revidiran**: 18. 03. 2026. I **Prihvać**en: 20. 03. 2026. I **Online First:** 30. 03. 2026.

Medicinska istraživanja 2026